Chemistry–A European Journal
Research Article
doi.org/10.1002/chem.202301439
Chemistry Europe
European Chemical Societies Publishing
www.chemeurj.org

The Role of Conjugation in the Halogen–Lithium Exchange Selectivity: Lithiation of 4,6,7,9-Tetrabromo-1,3-dimethyl-2,3-dihydro-1*H*-perimidine

Artyom A. Yakubenko,[b] Elena Yu. Tupikina,[b] and Alexander S. Antonov*[a]

This paper is dedicated to Professor Alexander F. Pozharskii on the occasion of his 85th birthday

Abstract: The first case of successful suppression of the coordination of a lithium atom with a dialkylamino group by the effective conjugation of the latter with the aromatic core has been discovered. This effect controls regioselectivity of the bromine–lithium exchange in 4,6,7,9-tetrabromo-1,3-dimethyl-2,3-dihydro-1*H*-perimidine, which leads to products with the most effective conjugation. As a result, the product of this quadruple exchange demonstrates no tendency of the coordination of the NMe groups to neighboring lithium atoms despite the absence of steric restrictions. Experimental results are explained by means of quantum chemical calculations: geometry optimization, natural bond analysis and scans using the modredundant scheme.

Introduction

Modern organic synthesis has reached an extraordinary level of sophistication, largely due to the advances of organometallic chemistry. Thus, the discovery of effective catalytic processes involving transition metals has given chemists powerful synthetic tools, such as cross-couplings, click reactions, stereoselective transformations and many others.[1–3] Despite the grand success of homogeneous catalysis, the high cost of palladium, platinum, gold, iridium etc., the necessity to use complicated (and expensive) ligands, and the difficulties with the purification of the final products from toxic transition metals still limit its application. The main group organometallics, such as organoaluminums, organoborons, Grignard reagents and organolithiums generally lack these disadvantages. That is why they not only keep their solid positions as indispensable tools for modern organic synthesis but also improve it with more and more novel applications discovered in recent years.[4,5] This stimulates the search for new regioselective methods of the synthesis of organometallic reagents. In the field of organolithiums, the halogen–lithium exchange nowadays regains its status as one of the most important and versatile methods for synthesis.[6] There is no surprise that to date, different features of this process, such as the influence of directing groups and the possibility of multiple halogen exchanges, were thoroughly investigated in a benzene series. Thus, it has been demonstrated that the presence of heteroatomic groups able to coordinate metal (so-called directing groups) facilitate the halogen exchange in the *ortho*-position, thus allowing regioselective functionalization (Scheme 1a).[7–10]

In the naphthalene series, these features are much less investigated, while the rigidity of a naphthalene ring significantly elevates the impact of the steric strain. In our recent paper, we have shown that the directing effect of dimethylamino groups in **1** can be completely suppressed by the steric strain of the molecule (Scheme 1b).[11]

It was also found that charge overload also significantly controls the regioselectivity of multiple halogen exchanges. For example, upon treatment of **1** with 2 equivalents of *n*-BuLi, no signs of simultaneous exchange of two halogen atoms in one ring were observed due to the disadvantageous charge overload (Scheme 1c).[11] This effect also prevents multiple halogen substitutions in the benzene series. Even though the formation of hexalithiobenzene is possible, it requires 24 equiv. of *tert*-BuLi, for instance.[12,13]

To date, three main effects are known to control the regioselectivity of the halogen–lithium exchange: the presence of the directing group, steric strain and the effectiveness of an "electron sink" (the possibility to utilize excess electrons). Here we present a "new player" in this competition for regioselectivity – the conjugation of an electron-donating group with an aromatic system – and its manifestation in bromine–lithium exchanges in 4,6,7,9-tetrabromo-1,3-dimethyl-2,3-dihydro-1*H*-perimidine **2**.

[a] *Dr. A. S. Antonov*
Institute of Organic Chemistry
University of Regensburg,
D-93053 Regensburg (Germany)
E-mail: alexander.antonov@chemie.uni-regensburg.de
[b] *A. A. Yakubenko, Dr. E. Y. Tupikina*
Institute of Chemistry
St. Petersburg State University
198504 St. Petersburg (Russian Federation)

Supporting information for this article is available on the WWW under https://doi.org/10.1002/chem.202301439

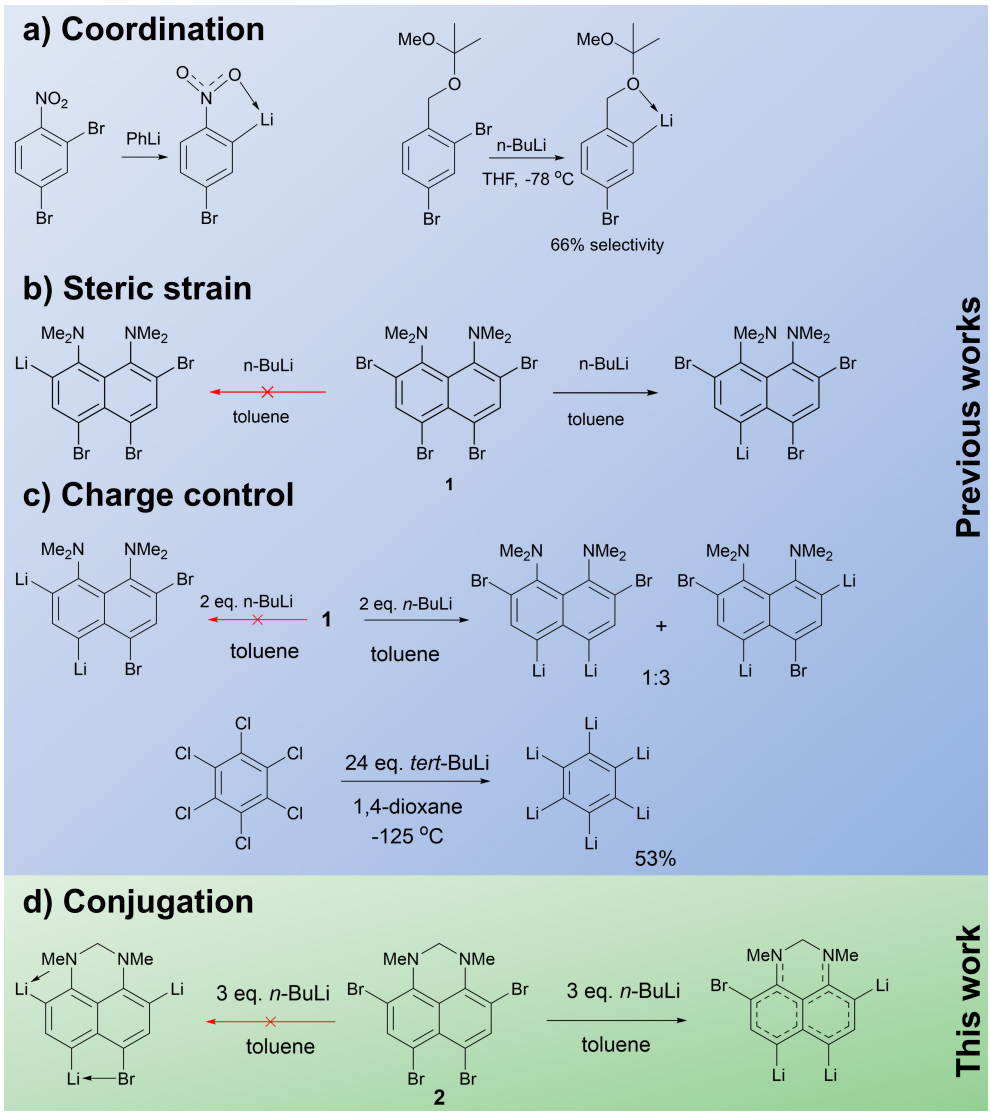

Scheme 1. Factors contributing to the Br→Li exchange regioselectivity.

Results and Discussion

Previously, we reported the formation of **2** as admixture during the synthesis of **1**.[11] In order to obtain **2** with reasonable yield, we investigated the oxidation of **1** with NBS in THF (Scheme 2). It was found that the reaction outcome significantly depends on the temperature. Thus, at 25 °C, only **2** and **3** are observed in the reaction mixture with 31% and 44% isolated yields, respectively. Demethylation of 1,8-bis(dimethylamino)naphthalene is known to occur in the presence of nucleophiles,[14] however, in our case, this transformation is rather radical in nature. Since NBS is a well-known oxidant, we believe that **2** is formed during the oxidation of **3** with NBS. Indeed, the elevation of the reaction temperature to 40 °C

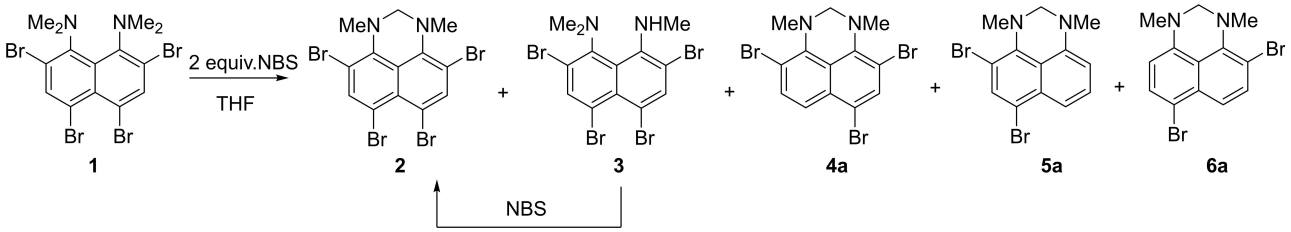

Scheme 2. Oxidation of **1** with NBS.

leaves only traces of **3** and makes **2** the main product with 42% isolated yield. Surprisingly, the debrominated products **4a**–**6a** are also formed under these conditions (Figure 1). Unfortunately, it is possible to obtain **5a** and **6a** only as an inseparable mixture with 19% total yield and a **5a**:**6a** ratio of 6.7:1. Refluxing **1** with two equivalents of NBS in THF facilitates debromination and leads to the formation of **4a** with 29% yield. Despite the complicity of this reaction, the formation of **4a**–**6a** was extremely useful for the further investigation of the bromine–lithium exchange. In contrast to previously studied diamine **1**, dihydroperimidine **2** has less conformational mobility of amino groups, opposite orientation of lone pairs of nitrogen atoms (*in,out* in **1** vs *out,out* in **2**) and dramatically smaller torsion distortion (Figures 2 and 3). The influence of this combination of structural parameters on the bromine–lithium permutation was investigated by treatment of **2** with *n*-BuLi under different conditions. The step-by-step lithiation of **2** can give two monolithioderivatives **4b** and **12b**, four dilithiospecies **5b**, **6b**, **10b** and **11b**, two trilithioderivatives **8b** and **9b** and finally tetralithioderivative **7b** (Scheme 3). Formed lithiated species were trapped by quenching with MeOH and the resulting mixture of products was studied by ^{1}H NMR spectroscopy (Table 1).

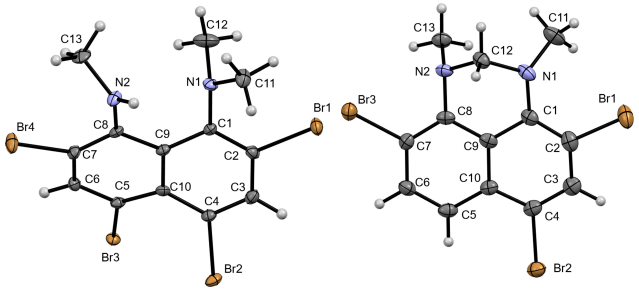

Figure 1. X-ray structures of **3** (left) and **4a** (right).

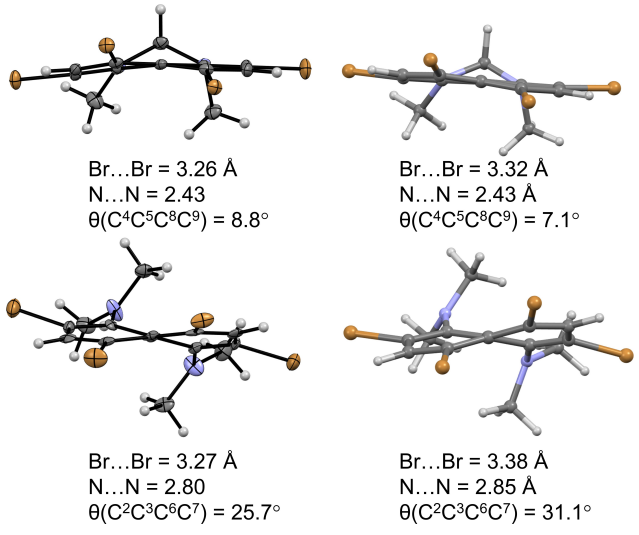

Figure 2. Experimental X-ray (left) and calculated in a vacuum (right) structures of **2** (top) and **1** (bottom). Selected geometric parameters are given.

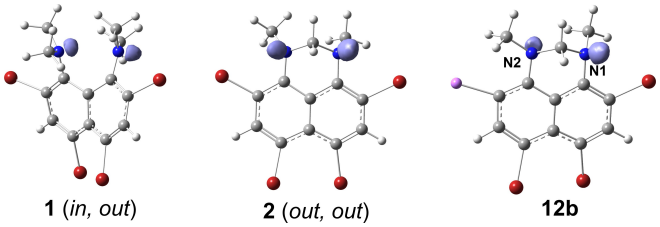

Figure 3. Electron localization function (ELF) isosurfaces (isovalue 0.85) for **1**, **2** and **12b** in the region of lone pairs of nitrogen atoms, other ELF regions are omitted for clarity.

We have found that the treatment of **2** with 0.9 equiv. of *n*-BuLi at −20 °C for 1 h and further quenching with MeOH leads to the formation of both **12a** and **4a** with a ratio of 1:2.5 together with some traces of **6a** (Table 1, entry 1). Increasing the temperature to 25 °C or the reaction time to 24 h does not noticeably affect the result (entries 2 and 3). Altogether, the first

All experiments were performed in toluene, since it provides fine solubility of lithiated species, stays liquid in a wide range of temperatures and has a low CH-acidity. In some cases, benzene was used as a less CH-acidic solvent. When it was possible, products were separated to confirm their structure. Further analysis of reaction mixtures was performed by comparing the chemical shifts of the NMe and NCH_2N groups' protons with our and literature data (Figure 4).[15] The geometries and energies of studied lithiated species were calculated for their sandwich-like complexes with toluene, in which each lithium atom is coordinated to one toluene molecule (Figure 5).

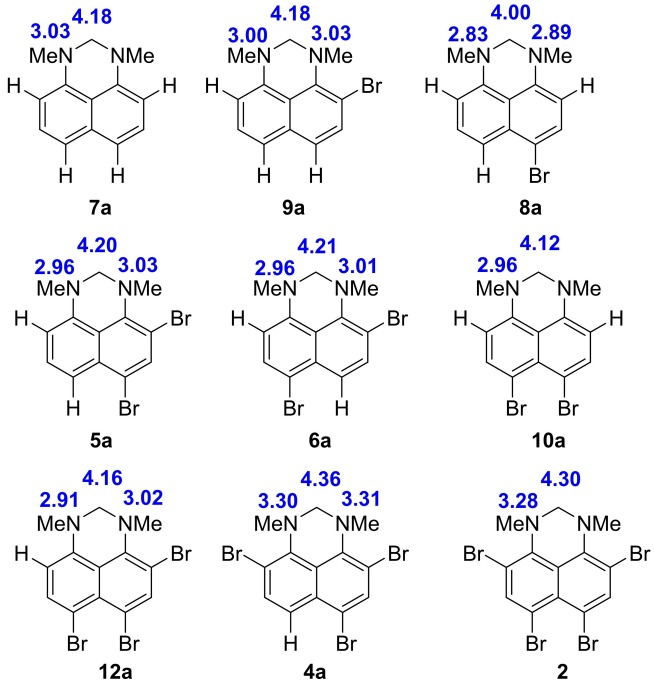

Figure 4. Chemical shifts (ppm) of the alkylamino groups' protons of 1,3-dimethyl-2,3-dihydro-1*H*-perimidine and its known bromoderivatives in $CDCl_3$.

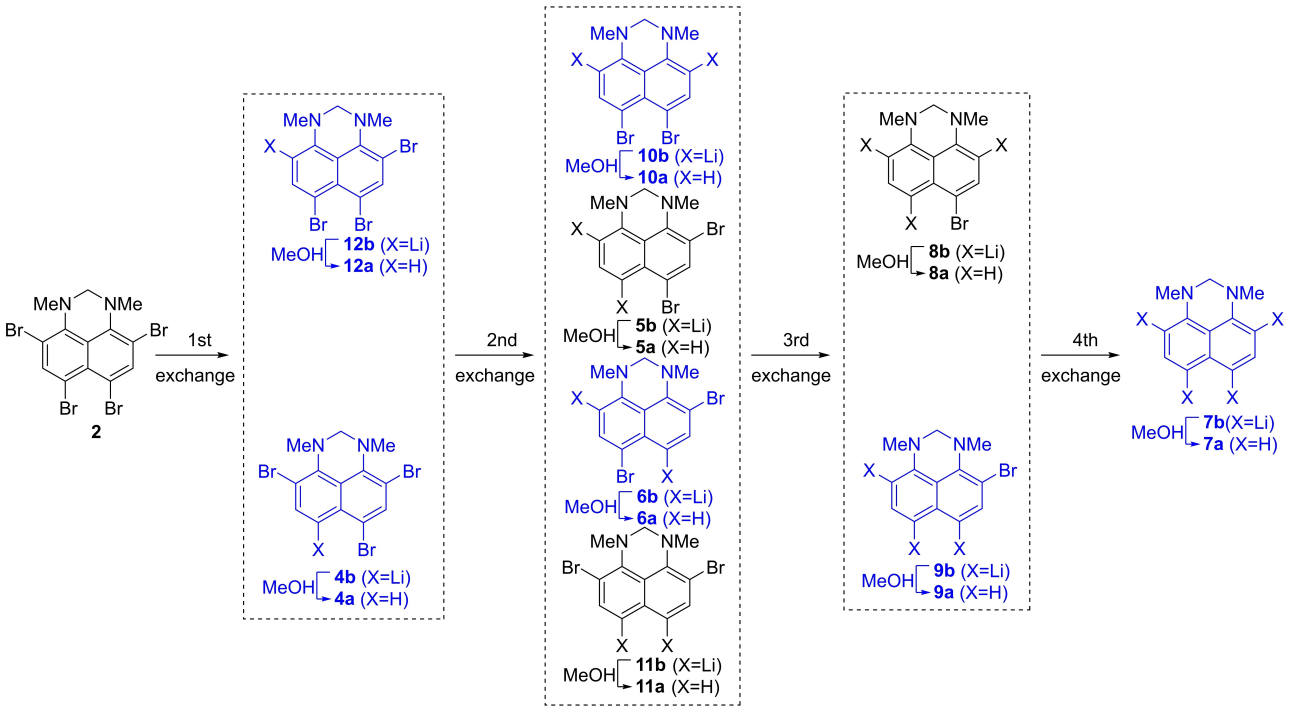

Scheme 3. Possible pathways of the step-by-step bromine–lithium exchange in **2**. Experimentally observed species are marked with blue.

Table 1. The composition of the reaction mixture after treatment of **2** with *n*-BuLi under different conditions and further quenching of the resulting naphthyllithiums with MeOH.

Entry	Solvent	*n*-BuLi, equiv.	Temp., °C	Time, h	Relative ratio of products						
					2	**12a**	**4a**	**10a**	**6a**	**9a**	**7a**
1	toluene	0.9	−20	1	1.6	0.4	1.0	–	0.1	–	–
2	toluene	0.9	25	1	1.9	0.4	1.0	0.1	0.1	–	–
3	toluene	0.9	−20	24	1.4	0.3	1.0	–	0.1	–	–
4	toluene	1.5	−20	1	0.2	0.7	1.0	0.3	0.3	–	–
5	toluene	1.5	25	1	0.1	0.2	1.0	–	0.2	–	–
6	toluene	2.8	−20	1	–	0.3	1.0	1.2	1.6	–	–
7	toluene	2.8	25	1	–	1.6	1.0	2.4	3.3	–	–
8	toluene	4.1	−20	1	–	–	1.0	2.8	3.6	2.3	0.1
9	toluene	4.1	25	1	–	–	–	0.5	0.7	1.0	0.1
10	toluene	8.1	−20	1	–	–	–	0.2	0.2	1.0	0.1
11	toluene	8.1	25	1	–	–	–	–	–	1.0	0.5
12	toluene	8.1	25	2	–	–	–	–	–	1.0	0.5
13	toluene	8.1	25	4	–	–	–	–	–	1.0	0.5
14	toluene	8.1	25	24	–	–	–	–	–	1.0	0.7
15	benzene	8.1	25	24	–	–	–	–	–	1.0	1.1
16	benzene	8.1	25	24	–	–	–	–	–	1.0	0.3
17	benzene	16.0	25	24	–	–	–	–	–	1.0	2.8

bromine–lithium exchange in **2** is not selective and leads to the formation of both possible products **12b** and **4b**.

It should be noted here that the first bromine–lithium exchange in **1** occurs selectively in *para*-position due to the coordination of the lithium atom to the *peri*-bromine atom, resulting in a significant decrease of naphthalene ring twisting ($\Delta\theta \approx 8°$).[11] Despite the similar $\Delta\theta \approx 6°$ value, the first exchange in **2** is not selective. It is very tempting to assume that *out,out*-conformation of amino groups facilitates the coordination of the lithium atom in *ortho*-position, thus bringing thermodynamic stabilization. However, the optimized geometry of **12b** (Figure 5) demonstrates no such coordination – neither in the presence nor the absence of the toluene saturating coordination demands of lithium. Moreover, the visualization of electron localization function (ELF) and NBO-analysis clearly demonstrate that a lone pair of N2 atom is involved in the conjugation with the aromatic system and effectively interacts with C–C antibonding σ* orbitals: the energy of this interaction for the N2 orbital is 27.8 kcal/mol and for N1 orbital is 11.2 kcal/mol (Figures 3 and 6).

Altogether, the exchange of bromine in *ortho*-position leads to the formation of **12b** and removes steric pressure on the

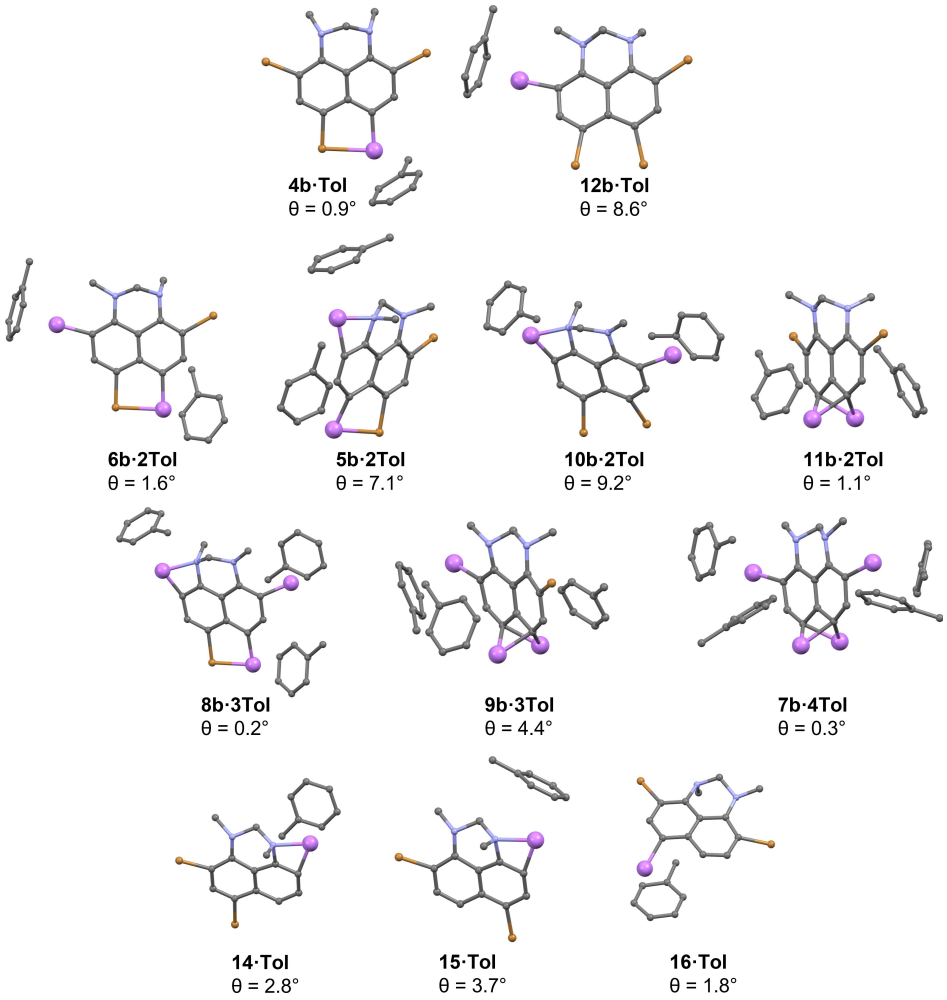

Figure 5. Optimized geometries of studied lithiated species – B3LYP–D3/6-311++G(d,p). θ($C^4C^5C^8C^9$) values are given. Hydrogen atoms are omitted for clarity.

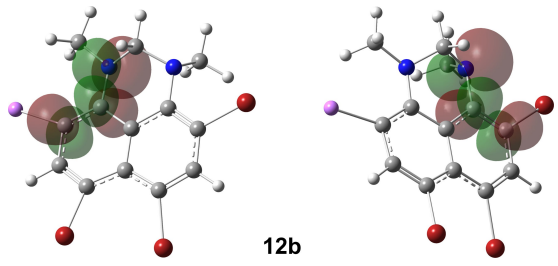

Figure 6. Natural bond orbitals (NBO) for **12b·Tol**. Overlapping of lone pair of N2 nitrogen and C–C antibonding σ* orbital (left), lone pair of N1 nitrogen and C–C antibonding σ* orbital (right). The isovalue for orbitals visualization is 0.02. Toluene molecules are omitted for clarity.

neighboring amino group. This allows its effective conjugation, which successfully competes with the planarization of the naphthalene ring and the coordination of bromine to lithium in the case of **4b** formation.

To our knowledge, this is the first manifestation of this effect in *ortho*-lithioanilines. The reason is that this effect is generally "hidden" behind a much stronger coordination of the directing group to the lithium atom. Thus, according to our quantum chemical calculations, the rotation of the NMe_2 group in 2-lithio-*N,N*-dimethylaniline complex with toluene first leads to a slight increase of the electronic energy with a maximum of +0.6 kcal/mol at approximately 30° (Figure 7). Further rotation leads to the stabilization via coordination of nitrogen to lithium with up to −6.8 kcal/mol at 120°. In total, the loss in conjugation energy is negligibly small and does not affect the halogen–lithium exchange in simple anilines and becomes noticeable only in strained substrates like **12b**. Thus, a similar rotation of the N(2)Me group in **12b·Tol** leads to the dramatically higher increase of the electronic energy with a maximum of +7.4 kcal/mol at approximately 75° and further coordination to the lithium atom brings a stabilization of only 2.9 kcal/mol at 80° (Figure 8). Further rotation forces the inversion of the N(1)Me group, allowing its effective conjugation with the aromatic core, which noticeably stabilizes the system but nevertheless leaves the process thermodynamically unfavorable.

The removal of the repulsion of *peri*-bromine atoms upon transition to tribromoderivative **13** elevates the impact of

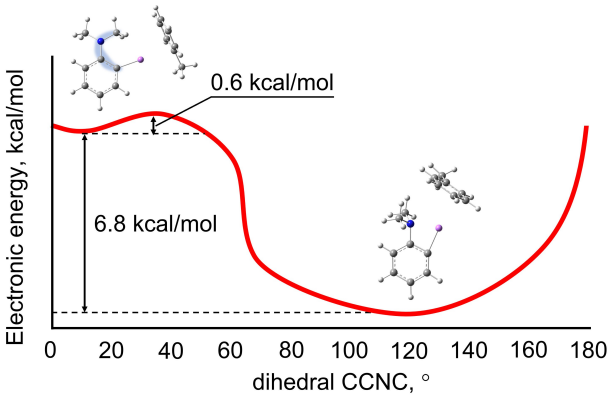

Figure 7. Dependence of relative electronic energy on the dihedral angle of the CCNC for the complex for 2-lithio-*N*,*N*-dimethylaniline with toluene, scan along CCNC using the modredundant scheme.

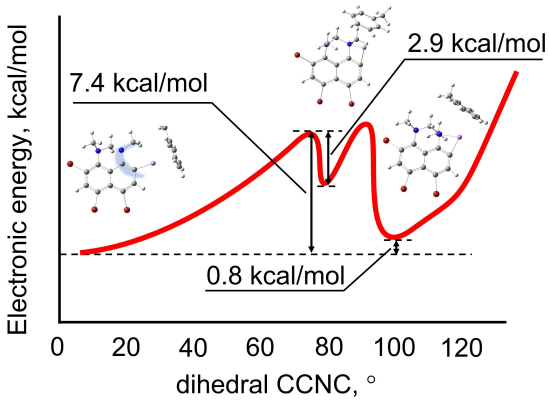

Figure 8. Dependence of the relative electronic energy on the dihedral angle of the CCNC for **12b·Tol**, scan along CCNC using the modredundant scheme.

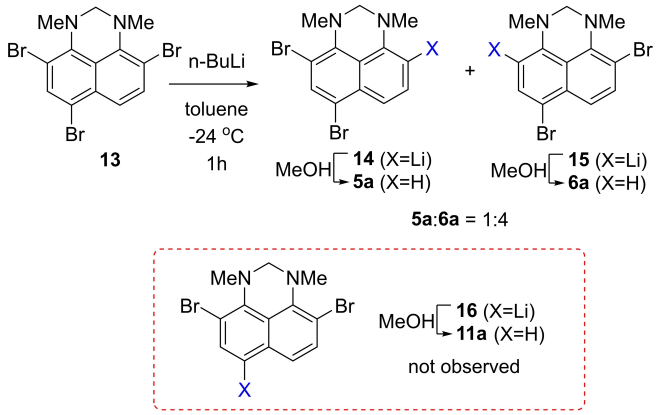

Scheme 4. Bromine–lithium exchange selectivity in **13**.

conjugation on the regioselectivity of the bromine–lithium exchange. Thus, treatment of **13** with 0.9 equiv. of *n*-BuLi leads only to the formation of *ortho*-lithioderivatives **14** and **15** with the ratio 1:4, while no formation of **16** is observed (Scheme 4).

While the N2 atom in compounds **14** and **15** participates in the coordination of lithium, the unshared electron pair of N1 effectively conjugates with the aromatic system (E = 38.6 and 37.7 kcal/mol in **14** and **15** respectively, Figure 9). Despite the highest distortion of the molecule of **15** caused by the repulsion of the bromine atom and methyl group ($\theta = 3.7°$), the conjugation leads to the highest thermodynamic stability of **15** among isomers: $\Delta G(\mathbf{15}\rightarrow\mathbf{14}) = +0.9$ kcal/mol, $\Delta G(\mathbf{15}\rightarrow\mathbf{16}) = +4.3$ kcal/mol.

Treatment of **2** with 1.5 equiv. of *n*-BuLi at −24 °C and further quenching with MeOH leads to the formation of **6a** and **10a** together with **4a** and **12a** after quenching the reaction mixture with MeOH, no formation of **5a** and **11a** was observed (Table 1, entry 4). Elevating the temperature to 25 °C gives poorly reproducible but overall similar results (entry 5). Analysis of orbitals interactions of corresponding lithiated species clearly demonstrates that the most effective conjugation for both nitrogen atoms occurs in **11b** (Figure 10). Nevertheless, corresponding bromide **11a** is not observed in the reaction mixture, since this interaction is outweighed by the better saturation of the coordination sphere of lithium in **5b**, **6b** and **10b**. Meanwhile, the charge overload in one ring of **5b** makes it significantly less stable: $\Delta G(\mathbf{10b}\rightarrow\mathbf{5b}) = +6.3$ kcal/mol (Figure 11). The combination of the abovementioned factors makes **6b** and **10b** the most thermodynamically stable isomers ($\Delta G(\mathbf{10b}\rightarrow\mathbf{6b}) = +1.9$ kcal/mol), which are observed in the reaction mixture in comparable amounts.

The triple and quadruple halogen exchange in **2** reveals the strongest manifestation of discussed effect. Thus, treatment of **2** with 2.8 equivalents of *n*-BuLi (entries 8 and 9) leads to the formation of **9b** as the only product of the triple halogen exchange. While **9b**, unlike isomeric **8b**, has no coordination of the amino group to the neighboring lithium atom, the gain of conjugation energy facilitates its formation. From the NBO analysis, one can clearly see that in the case of **9b**, both

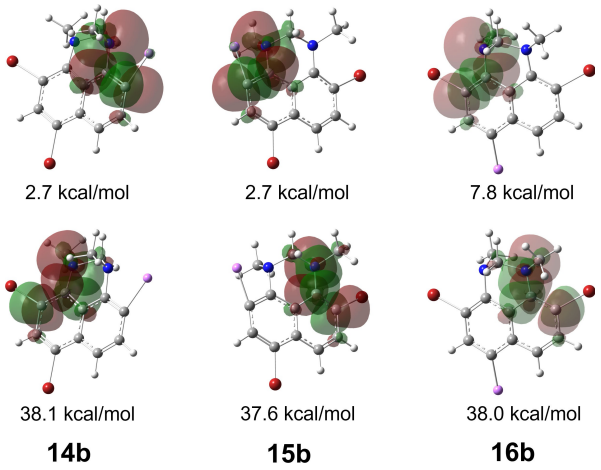

Figure 9. Natural bond orbitals (NBO) for **14b·Tol**, **15b·Tol**, **16b·Tol**. Overlapping of lone pair of N1 nitrogen and C–C antibonding σ* orbital (top), lone pair of N2 nitrogen and C–C antibonding σ* orbital (bottom). Isovalue for orbitals visualization is 0.02. Toluene molecules are omitted for clarity.

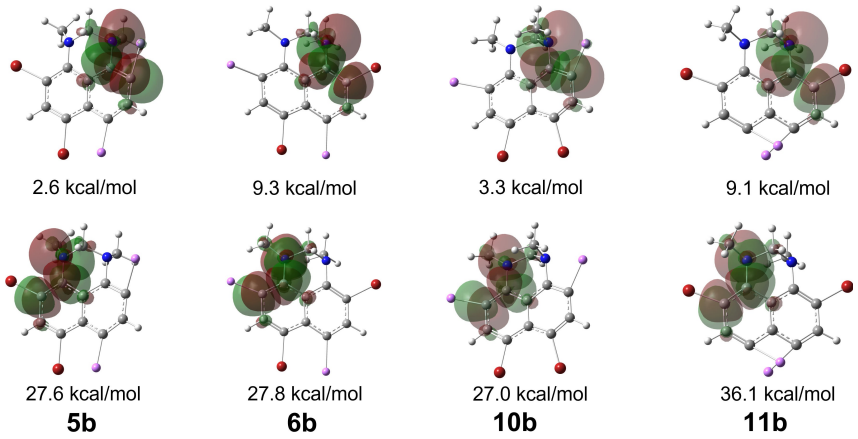

Figure 10. Natural bond orbitals (NBO) for **5b·2Tol**, **6b·2Tol**, **10b·2Tol**, **11b·2Tol**. Overlapping of lone pair of N1 nitrogen and C–C antibonding σ* orbital (top), lone pair of N2 nitrogen and C–C antibonding σ* orbital (bottom). Isovalue for orbitals visualization is 0.02. Toluene molecules are omitted for clarity.

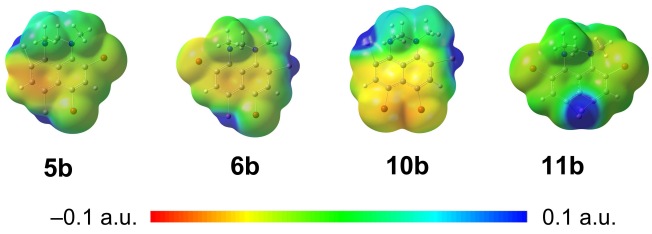

Figure 11. Isosurfaces of electron density (isovalue 0.001 a.u.) mapped by electrostatic potential for **5b·2Tol**, **6b·2Tol**, **10b·2Tol** and **11b·2Tol**. Toluene molecules are omitted for clarity.

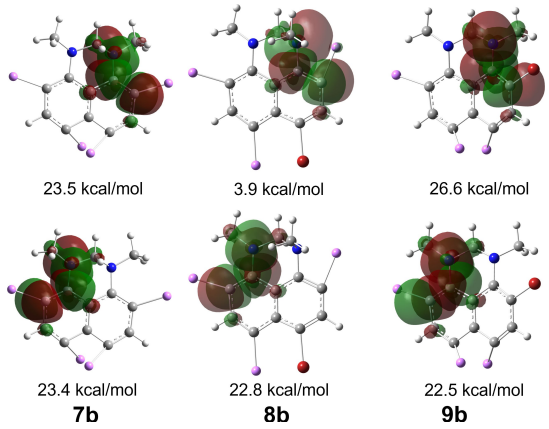

Figure 12. Natural bond orbitals (NBO) for **7b·4Tol**, **8b·3Tol**, **9b·3Tol**. Overlapping of lone pair of N1 nitrogen and C–C antibonding σ* orbital (top), lone pair of N2 nitrogen and C–C antibonding σ* orbital (bottom). The isovalue for orbitals visualization is 0.02. Toluene molecules are omitted for clarity.

nitrogen atoms are effectively conjugated with an aromatic core (Figure 12). In contrast, the triple exchange in **1** is not selective and leads to the formation of both possible isomers due to the much stronger impact of the N→Li coordination on the thermodynamic stabilization.

Finally, treatment of **2** with 4 and more equiv. of *n*-BuLi leads to the formation of **7b** (entries 8–16). The structure of the latter avoids the N→Li coordination in favor of the most effective conjugation of the lone pairs of both nitrogen atoms with the aromatic system (Figure 12).

Polylithionapthalenes are rather attractive substrates for the preparation of polyfunctionalized rigid organic compounds. In order to demonstrate the reactivity of **7b** towards nucleophiles we treated it with Me_2S_2. As a result, tetrakismethylthio derivative **17** was obtained with good yield (Scheme 5, Figure 13).

Conclusions

In summary, the first case of effective competition of the conjugation of an alkylamino group with an aromatic system

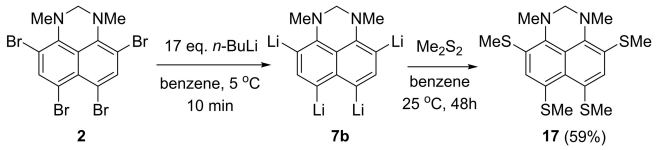

Scheme 5. Synthesis of **17**.

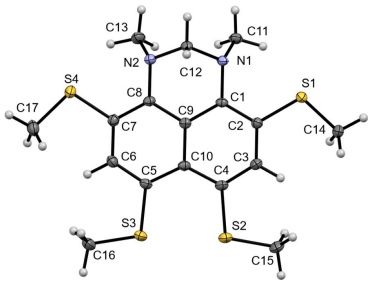

Figure 13. X-ray structure of **17**.

against the saturation of the coordination sphere of a lithium atom has been discovered. The manifestation of this effect significantly affects the regioselectivity of the bromine–lithium exchange in 4,6,7,9-tetrabromo-1,3-dimethyl-2,3-dihydro-1*H*-perimidine as well as the structure of lithiated products. The first exchange is not selective and leads to the formation of both possible products. While the 6-lithioderivative is stabilized by the reduction of steric strain and the coordination of the lithium atom by bromine, the formation of 4-lithioderivative is facilitated by the dramatic improvement of the effectiveness of the conjugation of the amino nitrogen with the naphthalene core. The selectivity of the second exchanges is controlled by the combination of the abovementioned conjugation effect, coordination of the NMe group to the lithium atom, steric strain and effective charge distribution. The third exchange is mainly influenced by the effective conjugation of both nitrogen atoms with the aromatic core, making the 4-bromo-6,7,9-trilithioderivative the only product. In most cases, effective conjugation outweighs the tendency of the amino group to coordinate with the neighboring lithium atom. As a result, the product of a quadruple exchange – 4,6,7,9-tetralithio-1,3-dimethyl-2,3-dihydro-1*H*-perimidine – demonstrated no tendency in the participation of NMe groups in the saturation of the coordination sphere of neighboring lithium atoms.

Experimental Procedures

General

Toluene and benzene were dried over sodium/benzophenone.

Liquid-state NMR experiments were performed using a Bruker Avance iii NMR spectrometer (400 MHz for ^{1}H and 100 MHz for ^{13}C) at the Center for Magnetic Resonance, St. Petersburg State University Research Park. Chemical shifts are referenced to TMS for ^{1}H and ^{13}C.

HR-ESI mass-spectra were obtained on a BRUKER maXis spectrometer equipped with an electrospray ionization (ESI) source; methanol was used as the solvent at the Chemical Analysis and Materials Research Centre, St. Petersburg State University Research Park. The instrument was operated in positive mode using an m/z range of 50–1200. The capillary voltage of the ion source was set at 4000 V. The nebulizer gas pressure was 1.0 bar, and the drying gas flow was set to 4.0 L/min.

Single crystals of **3** were grown by slow evaporation of pentane solution at −20 °C, while crystals of **4a** were grown by slow evaporation of an ethyl acetate solution and crystals of **17** were grown from the mixture of diethyl ether and hexane at RT in the dark. The single crystal X-ray diffraction data were collected using the SuperNova diffractometer equipped with a HyPix-3000 detector and a micro-focus Cu Ka radiation source (λ = 1.54184 A) at temperature T = 100 (2) K at the Centre for X-ray Diffraction Studies, St. Petersburg State University Research Park. Using Olex2,[16] the structure was solved with the SHELXT[17] structure solution program using Intrinsic Phasing and refined with the SHELXL[18] refinement package using Least Squares minimization. Empirical absorption correction was applied in CrysAlisPro[19] program complex using spherical harmonics, implemented in SCALE3 ABSPACK scaling algorithm.

Computations

Computational resources were provided by the Computer Center of Saint-Petersburg University Research Park (http://www.cc.spbu.ru/). The calculations were carried out using the Gaussian16 software package.[20] Geometry optimizations (with standard convergence criteria for forces and displacements) and vibrational harmonic frequencies calculation were performed at the B3LYP/6-311++G(d,p) level of theory. The Grimme dispersion correction D3 with zero damping was included.[21] All structures were checked on the absence of imaginary vibrational frequencies. Solvent effects were accounted implicitly using the conductor-like polarizable continuum model (CPCM) and explicitly by adding toluene molecules in the first coordination sphere of lithium atom.

The MultiWFN[22] program was used for calculating the surfaces of electron density, electron localization function[23] and molecular electrostatic potential.[24] NBO analysis performed using NBO 7.0 program. The visualization was performed using GaussView and Matlab R2021b.

Synthesis

*2,4,5,7-Tetrabromo-1,8-bis(dimethylamino)naphthalene (**1**).* 4,5-dibromo-1,8-bis(dimethylamino)naphthalene.[11]

(470 mg, 1.26 mmol), NBS (472 mg, 2.65 mmol) and cooled to −20 °C THF (20 mL) were placed in a flask. The reaction mixture was stirred overnight at −20 °C. The solvent was removed in vacuo to form dark-orange waxy residue. 10% aqueous ammonia solution (25 mL) was added to the residue. The product was extracted with dichloromethane (3×15 mL). Organic layers were combined and dried over anhydrous sodium sulfate. The solvent was removed in vacuo. The residue was recrystallized from petroleum ether to yield **1** as orange crystals (583 mg, 87%) with mp 151–152 °C.

^{1}H NMR ($CDCl_3$, 400 MHz): $\delta = 7.89$ (s, 2H), 2.96 (s, 12H). ^{13}C NMR ($CDCl_3$, 100 MHz): $\delta = 147.08$, 138.01, 134.84, 131.74, 119.89, 114.51, 44.34.

*2,4,5,7-Tetrabromo-N^1,N^1,N^8-trimethylnaphthalene-1,8-diamine (**3**).* The mixture of **1** (100 mg, 0.19 mmol), NBS (71 mg, 0.40 mmol) and THF (15 mL) was stirred overnight at room temperature. The solvent was removed in vacuo to form dark-orange waxy residue. 10% aqueous ammonia solution (20 mL) was added. The product was extracted with dichloromethane (3×10 mL). Organic layers were combined and dried over anhydrous sodium sulfate. The solvent was removed in vacuo. The residue was chromatographed on silica using benzene as eluent; greenish-yellow fraction with $R_f = 0.35$ was collected. The solvent was removed in vacuo to give **3** as greenish-yellow crystals (28 mg, 29%) with mp 72–74 °C.^{1}H NMR ($CDCl_3$, 400 MHz): $\delta = 8.84$ (s, 1H), 8.02 (s, 1H), 8.01 (s, 1H), 3.04 (s, 3H), 3.01 (s, 6H). ^{13}C NMR ($CDCl_3$, 100 MHz): $\delta = 148.78$, 145.49, 140.00, 139.30, 130.58, 130.39, 121.00, 118.43, 111.21, 109.68, 42.28, 37.00. HRMS (ESI): m/z $[M+H]^+$ calcd for $C_{13}H_{13}Br_4N_2^+$: 516.7766, 514.7786, 518.7745, 512.7807, 520.7725; found: 516.7768, 514.7795, 518.7748, 512.7850, 520.7723.

*4,6,9-tribromo-1,3-dimethyl-2,3-dihydro-1H-perimidine (**4a**).* The mixture of **1** (150 mg, 0.28 mmol), NBS (106 mg, 0.59 mmol) and THF (15 mL) was refluxed for 12 h. The solvent was removed in vacuo to form dark-orange waxy residue. 10% aqueous ammonia solution (20 mL) was added to the residue. The product was extracted with dichloromethane (3×10 mL). Organic layers were combined and dried over anhydrous sodium sulfate. The solvent was removed in vacuo. The residue was chromatographed on silica using a mixture of benzene/hexane 10:1 as eluent; colorless fraction with $R_f = 0.5$

was collected. The solvent was removed in vacuo to give **4a** as grayish crystals (35 mg, 29%) with mp 87–88 °C.

^{1}H NMR ($CDCl_3$, 400 MHz): δ = 7.90 (s, 1H), 7.68 (s, 2H), 4.36 (s, 2H), 3.31 (s, 3H), 3.30 (s, 3H). ^{13}C NMR ($CDCl_3$, 100 MHz): δ = 142.71, 142.44, 134.66, 132.85, 131.28, 124.71, 122.65, 115.25, 112.41, 110.05, 71.82, 43.52, 43.48. HRMS (ESI): m/z $[M+H]^+$ calcd for $C_{13}H_{12}Br_3N_2^+$: 434.8525, 436.8504, 432.8545, 438.8484; found: 434.8532, 436.8513, 432.8553, 438.8493.

*4,6,7,9-tetrabromo- (**2**), 4,6-dibromo- (**5a**) and 4,7-dibromo- (**6a**) 1,3-dimethyl-2,3-dihydro-1H-perimidines.* The mixture of **1** (750 mg, 1.42 mmol), NBS (529 mg, 2.97 mmol) and THF (150 mL) was stirred overnight at 40 °C. The solvent was removed in vacuo to form dark-orange waxy residue. 10% aqueous ammonia solution (25 mL) was added to the residue. The products were extracted with dichloromethane (3×15 mL). Organic layers were combined and dried over anhydrous sodium sulfate. The solvent was removed in vacuo. The residue was chromatographed on silica using benzene as eluent; colorless fraction with R_f = 0.55 (**5a** and **6a**) and light-yellow fraction with R_f = 0.6 (**2**) were collected. The solvent was removed in vacuo to give **2** as light-yellow crystals (305 mg, 42%) with mp 108–109 °C and inseparable 6.7:1 mixture of **5a** and **6a** as colorless oil (96 mg, 19%).

*Alternative approach for the synthesis of 4,6-dibromo- (**5a**) and 4,7-dibromo- (**6a**) 1,3-dimethyl-2,3-dihydro-1H-perimidines.* Crystals of **4a** (150 mg, 0.34 mmol) were placed in a flame-dried round-bottomed flask. Freshly distilled over sodium/benzophenone toluene was added (15 mL). The flask was filled with argon and closed with a septa cap. The mixture was kept at −20 °C for 10 min, and a 1.6 M solution of *n*-BuLi in hexanes (0.23 mL, 0.37 mmol) was added via syringe. The yellow mixture was kept at −20 °C for 1 h. Methanol (0.2 mL) was added to the reaction mixture. The solvent was removed in vacuo. The products were extracted with dichloromethane (3×10 mL). Organic layers were combined and dried over anhydrous sodium sulfate. The solvent was removed in vacuo. The residue was chromatographed on silica using benzene as eluent; colorless fraction with R_f = 0.6 was collected. The solvent was removed in vacuo to give inseparable 1:7.7 mixture of **5a** and **6a** as grayish oil (50 mg, 41%).

2. ^{1}H NMR ($CDCl_3$, 400 MHz): δ = 8.08 (s, 2H), 4.30 (s, 2H), 3.28 (s, 6H). ^{13}C NMR ($CDCl_3$, 100 MHz): δ = 142.90, 139.59, 128.44, 126.63, 112.60, 111.54, 70.82, 43.64. HRMS (ESI): m/z $[M+H]^+$ calcd for $C_{13}H_{11}Br_4N_2^+$: 514.7610, 512.7630, 516.7590, 510.7650, 518.7572; found: 514.7622, 512.7639, 516.7608, 510.7658, 518.7613.

5a. ^{1}H NMR ($CDCl_3$, 400 MHz): δ = 7.90 (s, 1H), 7.55 (d, J = 8.5 Hz, 1H), 7.49 (t, J = 8.0 Hz, 1H), 6.64 (d, J = 7.5 Hz, 1H), 4.20 (s, 2H), 3.03 (s, 3H), 2.96 (s, 3H). ^{13}C NMR ($CDCl_3$, 100 MHz): δ = 144.35, 143.01, 133.72, 132.35, 128.45, 120.25, 117.18, 116.37, 110.64, 105.10, 71.32, 40.86, 36.86.

6a. ^{1}H NMR ($CDCl_3$, 400 MHz): δ = 7.77 (d, J = 9.1 Hz, 1H), 7.67 (d, J = 9.1 Hz, 1H), 7.64 (d, J = 8.2 Hz, 1H), 6.45 (d, J = 8.2 Hz, 1H), 4.21 (s, 3H), 3.01 (s, 4H), 2.96 (s, 4H). ^{13}C NMR ($CDCl_3$, 100 MHz): δ = 143.98, 143.15, 131.98, 131.94, 130.80, 123.87, 120.77, 112.73, 109.55, 104.79, 71.32, 40.94, 36.67.

HRMS (ESI) (for both **5a** and **6a**): m/z $[M+H]^+$ calcd for $C_{13}H_{13}Br_2N_2^+$: 356.9420, 354.9440, 358.9399; found: 356.9427, 354.9444, 358.9417.

*4,6,9-tribromo- (**4a**) and 4,6,7-tribromo- (**12a**) 1,3-dimethyl-2,3-dihydro-1H-perimidines.* Crystals of **2** (100 mg, 0.19 mmol) were placed in a flame-dried round-bottomed flask. Freshly distilled over sodium/benzophenone toluene was added (10 mL). The flask was filled with argon and closed with a septa cap. The mixture was kept at −20 °C for 10 min, and a 1.6 M solution of *n*-BuLi in hexanes (0.13 mL, 0.21 mmol) was added via syringe. The yellow mixture was kept at −20 °C for 1 h. Methanol (0.2 mL) was added to the reaction mixture. The solvent was removed in vacuo. The products were extracted with dichloromethane (3×10 mL). Organic layers were combined and dried over anhydrous sodium sulfate. The solvent was removed in vacuo. The residue was chromatographed on silica using a mixture of benzene/hexane 10:1 as eluent; colorless fraction with R_f = 0.5 was collected. The solvent was removed in vacuo to give to give inseparable 9.4:1 mixture of **4a** and **12a** as grayish oil (37 mg, 45%).

12a. ^{1}H NMR ($CDCl_3$, 400 MHz): δ = 8.07 (s, 1H), 7.79 (d, J = 8.4 Hz, 1H), 6.45 (d, J = 8.5 Hz, 1H), 4.16 (s, 2H), 3.02 (s, 3H), 2.91 (s, 4H).

*4-bromo-1,3-dimethyl-2,3-dihydro-1H-perimidine (**9a**).* Crystals of **2** (100 mg, 0.19 mmol) were placed in a flame-dried round-bottomed flask. Freshly distilled over sodium/benzophenone toluene was added (10 mL). The flask was filled with argon and closed with a septa cap. The mixture was kept at −20 °C for 10 min, and a 1.6 M solution of *n*-BuLi in hexanes (1 mL, 1.6 mmol) was added via syringe. The bright-yellow mixture was kept at 25 °C for 1 h. Methanol (0.5 mL) was added to the reaction mixture. The solvent was removed in vacuo. The products were extracted with dichloromethane (3×10 mL). Organic layers were combined and dried over anhydrous sodium sulfate. The solvent was removed in vacuo. The residue was chromatographed on silica using benzene as eluent; colorless fraction with R_f = 0.5 was collected. The solvent was removed in vacuo to give **9a** as colorless crystals (24 mg, 46%) with mp 103–104 °C.

^{1}H NMR ($CDCl_3$, 400 MHz): δ = 7.69–7.54 (m, 2H), 7.46 (dd, J = 8.5, 7.6 Hz, 1H), 6.63 (d, J = 7.6 Hz, 1H), 6.40 (d, J = 8.2 Hz, 1H), 4.18 (s, 2H), 3.03 (s, 3H), 3.00 (s, 3H). ^{13}C NMR ($CDCl_3$, 100 MHz): δ = 144.58, 144.29, 132.75, 130.54, 128.16, 116.74, 115.73, 110.42, 104.34, 103.80, 70.23, 37.04, 36.89. HRMS (ESI): m/z $[M-H]^+$ calcd for $C_{13}H_{12}BrN_2^+$: 275.0178, 277.0158; found: 275.0183, 277.0164.

*2,4,5,7-Tetrakis(methylthio)-1,3-dimethyl-2,3-dihydro-1H-perimidine (**17**).* Crystals of **2** (100 mg, 0.19 mmol) were placed in a flame-dried round-bottom flask. Freshly distilled over sodium/benzophenone benzene was added (10 mL). The flask was filled with argon and closed with a septa cap. The mixture was kept at 5 °C for 10 min, and a 1.6 M solution of *n*-BuLi in hexanes (2 mL, 3.2 mmol) was added via syringe. The bright-yellow solution was kept at 25 °C for 24 h. Dimethyl disulfide (420 μL, 4.8 mmol) was added to reaction mixture. All further steps were done in the dark as the target compound is light-sensitive. Reaction mixture was kept at room temperature for 48 h and was added to water (100 mL). Organic layer was separated, and remains of the product were extracted with dichloromethane (3×10 mL). Organic layers were combined and dried over anhydrous sodium sulfate. The solvent was removed in vacuo. The residue was chromatographed on silica using dichloromethane as eluent; yellowish fraction (yellow-greenish fluorescence) with R_f = 0.5 was collected. The solvent was removed in vacuo. The residue was chromatographed on alumina using benzene as eluent; yellowish fraction (yellow-greenish fluorescence) with R_f = 0.9 was collected. The solvent was removed in vacuo to give **17** as pale-yellow crystals (44 mg, 59%) with mp 88–89 °C.^{1}H NMR ($CDCl_3$, 400 MHz): δ = 7.46 (s, 2H), 4.31 (s, 2H), 3.22 (s, 6H), 2.55 (s, 6H), 2.52 (s, 6H). ^{13}C NMR ($CDCl_3$, 100 MHz): δ = 140.34, 130.23, 129.91, 128.89, 125.19, 123.65, 71.47, 43.31, 21.59, 15.85. HRMS (ESI): m/z $[M+H]^+$ calcd for $C_{17}H_{23}N_2S_4^+$: 383.0739, 384.0772, 385.0697; found: 383.0731, 384.0739, 385.0699.

Supporting Information

NMR spectra and X-ray data for obtained compounds can be found in the Supporting Information.

Deposition Numbers 2227277 (for **3**), 2227276 (for **4a**), 2252223 (for **17**) contain the supplementary crystallographic data for this paper. These data are provided free of charge by the joint Cambridge Crystallographic Data Centre and Fachinformationszentrum Karlsruhe Access Structures service.

Acknowledgements

This work was supported by the Russian Science Foundation (project 21-73-10040). The authors thank Mr. Daniel Raith for proofreading the paper with regard to the English language. Open Access funding enabled and organized by Projekt DEAL.

Conflict of Interests

The authors declare no conflict of interest.

Data Availability Statement

The data that support the findings of this study are available in the supplementary material of this article.

Keywords: organolithiums · conjugation · coordination · regioselectivity · naphthalene

[1] L. Casella, in *Compr. Inorg. Chem. II* (Eds.: J. Reedijk, K. Poeppelmeier), Elsevier Ltd, **2013**, p. 803.
[2] L. C. Campeau, N. Hazari, *Organometallics* **2019**, *38*, 3–35.
[3] N. Z. Fantoni, A. H. El-Sagheer, T. Brown, *Chem. Rev.* **2021**, *121*, 7122–7154.
[4] A. E. H. Wheatley, M. Uchiyama, Eds., *Polar Organometallic Reagents: Synthesis, Structure, Properties and Applications*, John Wiley & Sons Ltd, Chichester, **2022**, p. 416.
[5] Z. Chai, W. X. Zhang, *Organometallics* **2022**, *41*, 3455–3477.
[6] J. Clayden, *Organolithiums: Selectivity for Synthesis*, ELSEVIER SCIENCE Ltd, Oxford, **2002**, p. 400.
[7] G. Voß, H. Gerlach, *Chem. Ber.* **1989**, *122*, 1199–1201.
[8] A. G. Avent, P. B. Hitchcock, G. J. Leigh, M. Togrou, *J. Organomet. Chem.* **2003**, *669*, 87–100.
[9] R. A. Murphy, M. P. Kung, J. Billings, H. F. Kung, *J. Med. Chem.* **1990**, *33*, 171–178.
[10] M. Murakata, T. Ikeda, N. Kimura, A. Kawase, M. Nagase, M. Kimura, K. Maeda, A. Honma, H. Shimizu, *Tetrahedron* **2017**, *73*, 655–660.
[11] A. A. Yakubenko, V. V. Karpov, E. Y. Tupikina, A. S. Antonov, *Organometallics* **2021**, *40*, 3627–3636.
[12] N. Rot, F. Bickelhaupt, *Organometallics* **1997**, *16*, 5027–5031.
[13] J. R. Baran, C. Hendrickson, D. A. Laude, R. J. Lagow, *J. Org. Chem.* **1992**, *57*, 3759–3760.
[14] V. A. Ozeryanskii, A. F. Pozharskii, M. G. Koroleva, D. A. Shevchuk, O. N. Kazheva, A. N. Chekhlov, G. V. Shilov, O. A. Dyachenko, *Tetrahedron* **2005**, *61*, 4221–4232.
[15] N. V. Vistorobskii, A. F. Pozharskii, *Zh. Org. Khim.* **1995**, *31*, 1074–1079.
[16] O. V. Dolomanov, L. J. Bourhis, R. J. Gildea, J. A. K. Howard, H. Puschmann, *J. Appl. Crystallogr.* **2009**, *42*, 339–341.
[17] G. M. Sheldrick, *Acta Crystallogr. Sect. A* **2015**, *71*, 3–8.
[18] G. M. Sheldrick, *Acta Crystallogr. Sect. A* **2008**, *64*, 112–122.
[19] CrysAlisPro, Agilent Technologies. Version 1.171.36.28., **2012**.
[20] Gaussian 16, Revision C.01, M. J. Frisch, G. W. Trucks, H. B. Schlegel, G. E. Scuseria, M. A. Robb, J. R. Cheeseman, G. Scalmani, V. Barone, G. A. Petersson, H. Nakatsuji, X. Li, M. Caricato, A. V. Marenich, J. Bloino, B. G. Janesko, R. Gomperts, B. Mennucci, H. P. Hratchian, J. V. Ortiz, A. F. Izmaylov, J. L. Sonnenberg, D. Williams-Young, F. Ding, F. Lipparini, F. Egidi, J. Goings, B. Peng, A. Petrone, T. Henderson, D. Ranasinghe, V. G. Zakrzewski, J. Gao, N. Rega, G. Zheng, W. Liang, M. Hada, M. Ehara, K. Toyota, R. Fukuda, J. Hasegawa, M. Ishida, T. Nakajima, Y. Honda, O. Kitao, H. Nakai, T. Vreven, K. Throssell, J. A. Montgomery, Jr., J. E. Peralta, F. Ogliaro, M. J. Bearpark, J. J. Heyd, E. N. Brothers, K. N. Kudin, V. N. Staroverov, T. A. Keith, R. Kobayashi, J. Normand, K. Raghavachari, A. P. Rendell, J. C. Burant, S. S. Iyengar, J. Tomasi, M. Cossi, J. M. Millam, M. Klene, C. Adamo, R. Cammi, J. W. Ochterski, R. L. Martin, K. Morokuma, O. Farkas, J. B. Foresman, D. J. Fox, Gaussian, Inc., Wallingford CT, **2016**.
[21] S. Grimme, J. Antony, S. Ehrlich, H. Krieg, *J. Chem. Phys.* **2010**, *132*, 154104.
[22] T. Lu, F. Chen, *J. Comput. Chem.* **2012**, *33*, 580–592.
[23] A. Savin, R. Nesper, S. Wengert, T. F. Fässler, *Angew. Chem. Int. Ed. Engl.* **1997**, *36*, 1808–1832.
[24] J. Zhang, *J. Chem. Theory Comput.* **2018**, *14*, 572–587.

Manuscript received: May 5, 2023
Accepted manuscript online: June 1, 2023
Version of record online: ■■, ■■

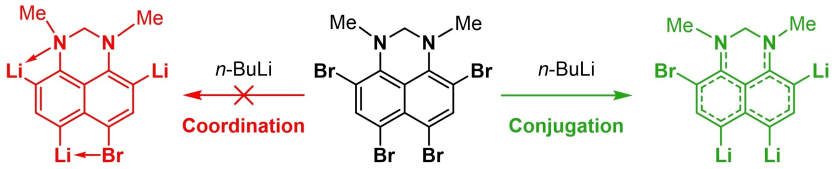

The first case of successful suppression of the coordination of a lithium atom with a dialkylamino group by the effective conjugation of the latter with the aromatic core has been discovered on the example of the bromine–lithium exchange in 4,6,7,9-tetrabromo-1,3-dimethyl-2,3-dihydro-1*H*-perimidine. Experimental results are explained by means of quantum chemical calculations.

*A. A. Yakubenko, Dr. E. Y. Tupikina, Dr. A. S. Antonov**